Journal of Power Sources 184 (2008) 245–250

Contents lists available at ScienceDirect

Journal of Power Sources

journal homepage: www.elsevier.com/locate/jpowsour

Studies of performance decay of Pt/C catalysts with working time of proton exchange membrane fuel cell

Zhen-Bo Wang[a,*], Peng-Jian Zuo[a], Xin-Peng Wang[b], Jie Lou[c], Bo-Qian Yang[b], Ge-Ping Yin[a]

[a] Department of Applied Chemistry, Harbin Institute of Technology, Harbin 150001, China
[b] Department of Physics, University of Puerto Rico, P.O. Box 23343, San Juan PR 00931, USA
[c] Department of Modern Physics, University of Science and Technology of China, Hefei 230026, China

ARTICLE INFO

Article history:
Received 21 April 2008
Received in revised form 9 June 2008
Accepted 9 June 2008
Available online 21 June 2008

Keywords:
PEMFC
Pt/C catalyst
Life test
Electrochemically active surface area
In situ CV study

ABSTRACT

Life test of the proton exchange membrane fuel cell (PEMFC) was carried out at a current density of 160 mA cm^{-2}. After an operation up to 2250 h, the performance of the single PEMFC shown by a current-time curve did not decay significantly. X-ray diffraction (XRD), scanning electron microscopy (SEM), and transmission electron microscopy (TEM) were employed to characterize both anodic and cathodic catalysts before and after the life test. Cyclic voltammetric (CV), polarization, and power density curves were plotted with the cell at different periods during long-term operation. The results showed that the electrochemically active surface areas (S_{EAS}) of anodic and cathodic catalysts firstly increased, and then decreased with the operation time. The S_{EAS} loss of anodic catalyst was evidently smaller than that of cathodic one. The thickness of Nafion® film decreased with working time as shown by SEM. The particle size of cathodic Pt/C catalyst was evidently bigger than that of anodic one. The degradation of cathodic catalyst for oxygen electroreduction was one of the main factors affecting the performance decay of PEMFC.

1. Introduction

Proton exchange membrane fuel cells (PEMFC) have been received significant development in the past decades as one of the main alternative power sources for stationary and mobile applications because of their high-power density, low weight, simplicity of operation, high-energy conversion efficiency, and zero harmful emissions [1,2]. The PEMFC stacks with electric powers of 1 kW, 2 kW, 5 kW, and 10 kW have been developed in different countries [3–8]. However, the cost of PEMFC stacks is too high for some applications, owing to the high cost of catalysts, which is one of the major obstacles for the broader commercialization of PEMFC [3,6]. Developments of high efficiency and low cost of catalytic materials are still being carried out. Generally, the relatively high cost of PEMFC stacks can be lowered if the durability of catalytic materials is prolonged. Many researches on PEMFC stacks with a long operation life have been conducted [9,10], but little progress has been made [11,12]. The main challenge is that the operating life is affected by the decay of fuel cell performance. During long-term operation the electrochemical performance is possibly degraded, and the service condition may be various. In order to understand the degradation mechanism, it is necessary to study the structural and chemical changes of each components affected by electrochemical stressing [13]. The state-of-the-art fuel cell electrodes are normally composed of carbon-supported noble metal, such as Pt as a catalyst, an ionic conductor, such as Nafion® [14,15], and a water-repelling agent, such as PTFE [16]. For these materials, some changes in catalytic and diffusion layers may have negative influence on the steady operation of PEMFC, including the sintering of Pt catalytic particles, the loss of catalytic active components, the poisoning of electrocatalysts caused by accumulated intermediates or impurities, the degradation of polymer electrolytic membrane, the change of hydrophobic/hydrophilic properties, etc. [17]. Among these the catalyst durability is still a challenge to develop PEMFC with an acceptable service life for transportation and stationary uses. The previous results indicated that the platinum catalyst particles were sintered during the test [18]. This was most likely because the available electrochemically active surface area of Pt catalyst decreased as the particles increased in size [19]. Pt sintering with a decrease of active surface area due to carbon-support corrosion and Pt dissolution/aggregation is considered to be one of the major factors causing the decay of cell performance [20]. Current research and development efforts are primarily focused on elucidating and quantifying catalytic degradation mechanism in order to determine whether carbon-supported platinum or platinum–alloy catalysts will meet

* Corresponding author at: Department of Applied Chemistry, Harbin Institute of Technology, No. 92 West Da-Zhi Street, Harbin 150001, China.
Tel.: +86 451 86417853; fax: +86 451 86413707.
E-mail address: wangzhenbo1008@yahoo.com.cn (Z.-B. Wang).

0378-7753/$ – see front matter © 2008 Elsevier B.V. All rights reserved.
doi:10.1016/j.jpowsour.2008.06.037

long-term performance requirements (e.g., for automotive applications $\leq 10\ \mu V\ h^{-1}$) [21], and then to develop more stable membrane electrode assembly (MEA) materials. Less work has been reported on the long-term stability of Pt/C catalysts used in PEMFC. Cyclic voltammetry (CV) has been frequently used to estimate the surface area (as electrochemically active surface area (EAS)) of Pt/C catalyst by adsorption–desorption of atomic hydrogen in acidic media [22,23]. In this paper, whether and how the catalyst degradation affects the long-term PEMFC performance is studied by *in situ* CV, X-ray diffraction (XRD), scanning electron microscopy (SEM), and transmission electron microscopy (TEM). The purpose of this study is to provide a better insight into the stability and changes of Pt/C catalysts under PEMFC operating conditions with CV and other techniques.

2. Experimental

2.1. MEA preparation

20 wt.% Pt/C (E-Tek Inc.) was used as catalysts for both electrodes. The catalyst and 5 wt.% Nafion® ionomer solution (DuPont EW = 1100) were mixed in isopropyl alcohol to form a homogeneous catalyst ink for the anode. The cathodic catalyst ink was composed of 20 wt.% Pt/C, Nafion® ionomer, and PTFE. The Nafion® contents in anodic and cathodic catalyst layers were 20 wt.%. The catalyst inks were deposited onto the gas diffusion layers (GDLs) by paint brush with a metal loading of 1 mg cm^{-2} for both electrodes. The carbon cloth (E-TEK, ELAT/NC/DS/V2 double sided ELAT electrode, carbon only, no metal, 20% wet proofed) was used as the GDL and backing layer. DuPont Nafion® 117 film was used as the solid electrolyte. Before being applied to the electrodes, the Nafion® membrane was pretreated by diluted nitric acid (the ratio of nitric acid/deionized water of 18 MΩ cm by volume is 1:1) at its boiling temperature for 20 min, and then rinsed five times with ultrapure water. The membrane was then immersed in the boiling ultrapure water for 1 h. The membrane electrode assembly (MEA) was formed by hot-pressing the anodic and cathodic diffusion layers onto the Nafion® film.

2.2. Electrochemical measurements

2.2.1. Single fuel cell tests

Tests of a single fuel cell were conducted by using a homemade 5 cm^2 apparent area test fixture. The fixture was composed of a pair of graphite plates with serpentine flow fields for reactants to flow. Hydrogen and air were used as the reactants with a flow rate of 100 mL min^{-1} at ambient pressure for the anode and the cathode, respectively. Both reactants were 100% humidified by passing them through humidifiers prior to entering the cell. The cell temperature was 45 °C. Rod-like heaters were inserted into the graphite plates to control the cell temperature. Polarization curves, power density curves, and potential–time curve were obtained by using a Fuel Cell Test Station (Scribner Associates Inc., Series 890B) in a galvanostatic polarization mode. Potential–time curve was measured at a current density of 160 mA cm^{-2} for 2250 h. To ensure that the electrolyte in the Nafion® membrane and electrode is moist enough to have high ionic conductivity, it is necessary to activate the MEA before the performance measurements. In the present experiment, the cell was conditioned with hydrogen and air by saturated humidification at 45 °C in a current density of 20 mA cm^{-2} for 24 h prior to the acquisition of life test data.

2.2.2. Cyclic voltammetry

In situ cyclic voltammograms [24,25] were obtained by using a PAR potentiostat/galvanostat (EG&G Model 273A) at a cell temperature of 25 °C. When CV of the anode was measured, the anode chamber was taken as a working electrode, and was purged with nitrogen gas, while the cathode chamber was fed with pure hydrogen at ambient pressure and it functioned as the counter and reference electrode which was defined as a dynamic hydrogen electrode (DHE). When CV of the cathode was measured, the cathode chamber was taken as a working electrode, and the anode served as the counter and reference electrodes. The potential was scanned (0.02 V s^{-1}) between 0.05 V and 1.2 V. All potential values presented in this work are versus DHE. Electrochemically active surface areas were calculated from integrated hydrogen adsorption and desorption of CV, and assuming a value of 210 μC cm^{-2} of Pt surface area for a monolayer coverage of hydrogen.

2.3. X-ray diffraction

XRD measurements for the catalyzed GDL were recorded on a Rigaku Ultima III X-ray diffractometer system (Rigaku MSC, Woodlands, TX) using a graphite crystal counter monochromator that filtered Cu $K\beta_{radiation}$. The X-ray source was operated at 40 kV and 40 mA. The pattern, recorded in a 2θ range of 20–90°, was obtained using high precision and high-resolution parallel beam geometry in a step scanning mode at 1° min^{-1}. Particle size was determined from the Scherrer equation using the Pseudo-Voigt profile function.

2.4. Scanning electron microscope

The thickness analyses of Nafion® films after and before test were performed with a scanning electron microscope (SEM, Hitachi Ltd., S-4700). Incident electron beam energies from 3 keV to 30 keV had been used. In all cases, the beam was at normal incidence to the sample surface and the measurement time was 100 s.

2.5. Transmission electron micrographs

Transmission electron micrographs for the catalyst samples were taken by a Japan JEOLJEM-2010EX transmission electron microscope with a spatial resolution of 1 nm. Before taking the electron micrographs, the catalyst samples were finely ground and ultrasonically dispersed in isopropyl alcohol, and a drop of the resultant dispersion was deposited and dried on a standard copper grid coated with a polymer film. The applied voltage was 100 kV with a magnification of 200,000× for the catalyst.

3. Results and discussion

Life test of single fuel cell was carried out at a temperature of 45 °C with a current density of 160 mA cm^{-2} for 2250 h. The potential–time curve is presented in Fig. 1. It can be seen that there are eight spikes in the curve. It was because the continuous discharge should be interrupted once for each 250 h of life test by refilling ultrapure water into the reactant humidifiers, which caused the performance of the PEMFC to recover its initial value of the discharge process for a few hours. The recovery is also attributed to the membrane humidification. The reactant humidifiers are not large enough in the present experiment. The Nafion® membrane is drying gradually during the operation due to the loss of ultrapure water in humidifiers. The ionic conductivity of ionomer membrane gradually lowers; thus its ohmic resistance gradually increases. The voltage across both sides of Nafion® membrane increases because of constant discharge current density. Namely, the voltage of fuel cell decays gradually with time. In each continuous discharge process, the majority of voltage loss occurs in initial hours and then its decline becomes less significant. Clearly, in the present life test, the performance of single cell does not markedly decay.

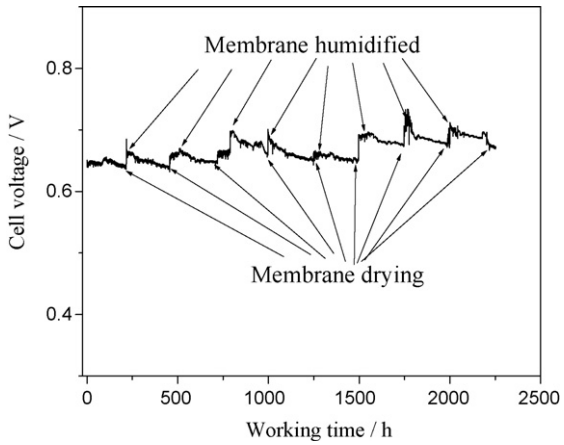

Fig. 1. Life test of a single PEMFC with an apparent area of 5 cm^2 and a Pt metal loading of 1 mg cm^{-2}. Operating at 45 °C with a current density of 160 mA cm^{-2}. Anode and cathode are fed with hydrogen and air, respectively, with a flow rate of 100 mL min^{-1} at ambient pressure.

Table 1
Comparison of open circuit voltages of PEMFC at different intervals

Working time (h)	OCV (V)
0	0.992
1000	1.006
1500	1.009
2000	1.018
2250	1.020

The open circuit voltages (OCVs) of a fuel cell at different test times are listed in Table 1. The OCVs were obtained after refilling ultrapure water into humidifiers prior to the next 250 h test. It can be seen that OCVs increase slightly with test time. Hydrogen peroxide (H_2O_2) is formed at the cathode due to inadequate reduction of oxygen [12,26]. The Nafion® membrane does not withstand H_2O_2 [12,26], and thins due to the corrosion by H_2O_2. However, the Nafion® film is not broken down after 2250 h during this experiment. The reaction gases do not permeate to the other electrode, and the mixed potential does not occur [10]. Hence, the OCVs of a fuel cell do not decrease with time.

Polarization curves and power density curves of PEMFC at different intervals are presented in Fig. 2. The initial maximum power density is 242 mW cm^{-2}, and then it increases up to 295 mW cm^{-2} after 2000 h of operation, and slightly decreases

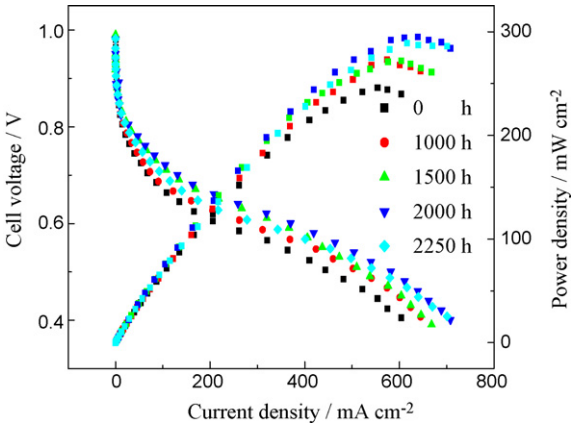

Fig. 2. Performance of a single PEMFC before test and at different intervals. Cell temperature: 45 °C. Anode and cathode are fed with hydrogen and air, respectively, with a flow rate of 100 mL min^{-1} at ambient pressure.

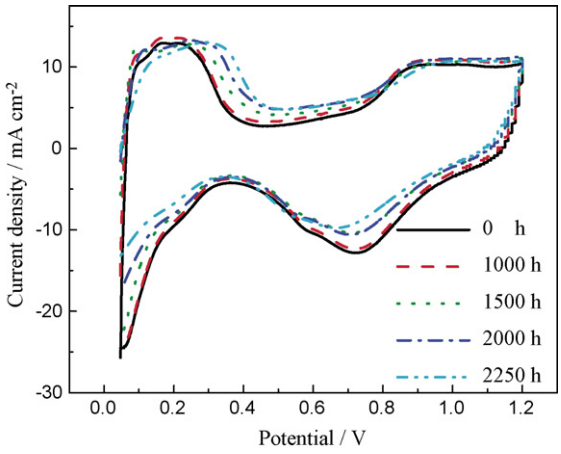

Fig. 3. CV curves of anodic Pt/C catalyst at different intervals during life test at 25 °C.

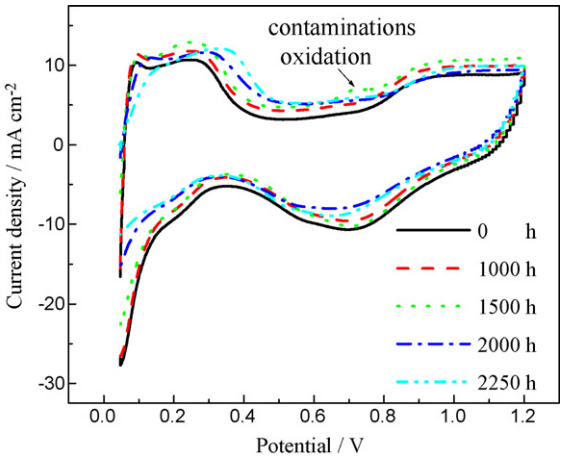

Fig. 4. CV curves of cathodic Pt/C catalyst at different intervals during life test at 25 °C.

down to 289 mW cm^{-2} after 2250 h of the test. The polarization decay with time of the fuel cell is similar to the power density change with time, i.e. first augments and then decreases.

Figs. 3 and 4 show the CV curves of anodic and cathodic catalysts for hydrogen adsorption–desorption at different intervals of the life test. The normal peaks of hydrogen adsorption–desorption on Pt/C catalysts are easily identified in Figs. 3 and 4 before life test. Namely, the two peaks occur at 0.125 V (weak adsorption hydrogen) and 0.275 V (strong adsorption hydrogen) during the anodic cycles corresponding to the stripping of adsorbed hydrogen. The flat region between 0.35 V and 0.60 V corresponds to the double layer region. The hydrogen adsorption–desorption regions on Pt/C cata-

Table 2
S_{EAS} and S_{XRD} area results of Pt/C catalysts before life test and at different intervals

Electrode	Working time (h)				
	0	1000	1500	2000	2250
Cathode					
S_{EAS} (m^2 g^{-1})	42.5	47.5	44.8	30.5	21.6
Changing rate (%)	–	+11.8	−5.7	−35.8	−54.5
Anode					
S_{EAS} (m^2 g^{-1})	53.6	55.7	50.8	46.3	38.9
Changing rate (%)	–	+3.9	−8.8	−16.9	−30.2
Catalyst					
S_{XRD} (m^2 g^{-1})	112.1	–	–	–	–

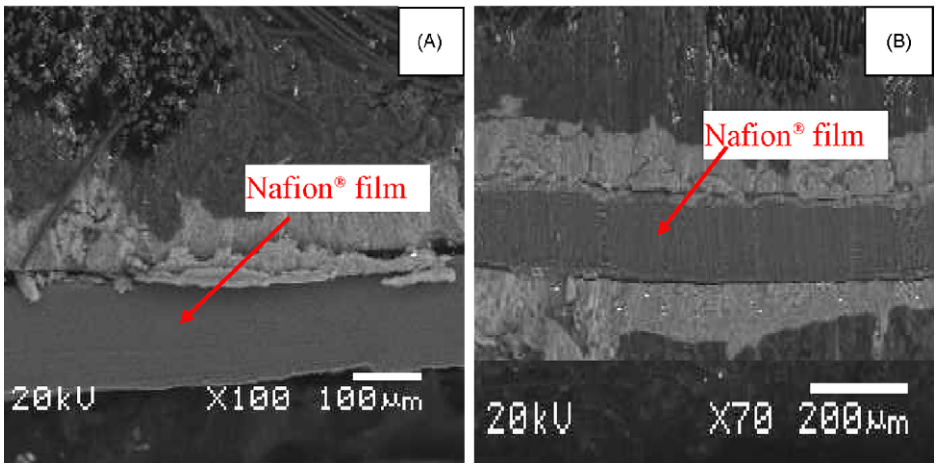

Fig. 5. SEM images of the MEAs prior to (A) and after (B) life test.

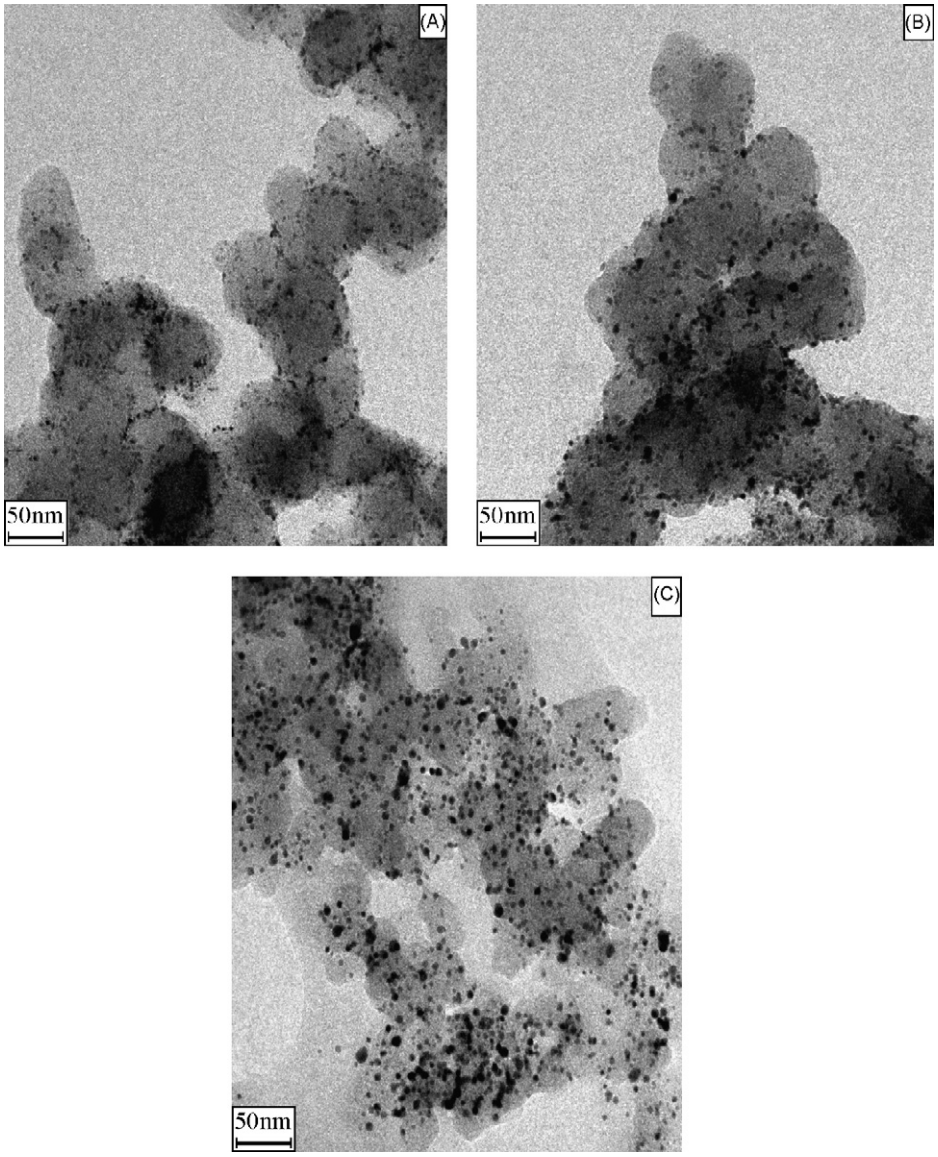

Fig. 6. TEM images of Pt/C catalysts before and after life test. (A) New Pt/C, before operation; (B) anodic Pt/C, after operation; (C) cathodic Pt/C, after operation.

lysts first increase and then decrease gradually with time. The mode of change is in good consistent with that of PEMFC performance. The two normal peaks of hydrogen desorption decay gradually with test time. The double layer capacities increase gradually with time.

The electrochemically active surface areas (S_{EAS}) of the catalysts are calculated with the recognized method based on the hydrogen adsorption–desorption curves by Eq. (1) [22,23] as follows:

$$S_{EAS} = \frac{Q_H}{G \times 210} \quad (1)$$

where Q_H is the charge quantity calculated from integrated in CV for hydrogen adsorption–desorption in microcoulomb (μC), G represents the loading of Pt metal (mg cm^{-2}) in the electrode, and 210 is the charge required to oxidize a monolayer of hydrogen on the Pt catalyst in μC cm^{-2} [22]. The S_{EAS} of anodic and cathodic catalysts are listed in Table 2.

The S_{EAS} of anodic and cathodic catalysts initially increase and then gradually decrease with test time as shown in Table 2. The S_{EAS} loss for the cathode and the anode after a test time of 2250 h are 54.5% and 30.2%, respectively. The degradation extent of S_{EAS} of cathodic catalyst is more obvious than that of anodic one. After the operation, the utilization of anodic catalyst decreases from 47.8% to 34.7%, and that of cathodic catalyst decreases from 37.9% to 19.3%. This result is in agreement with other groups' reports [19,27]. The decrease of utilization and S_{EAS} of cathodic catalyst is probably due to the higher water content, higher pH value, and higher oxygen concentration in the cathode than those in the anode. In addition, cathodic potential is much higher than anodic one during PEMFC operation. The change of polarization curves with time as shown in Fig. 2 lags that of S_{EAS} (Table 2). It could be resulted from the thickness change of Nafion® film as shown in Fig. 5. The average thickness of five measurements for each Nafion® film had the values of 175 μm and 171 μm before and after the life test, respectively. The Nafion® film was thinned by about 4 μm, while the standard error of such measurements is ±0.3 μm. This result is similar to that of Cho and coworkers [28] group by running PEMFCs for 500 or 1000 h. The decrease of thickness results in the increase of the ionic conductivity of the film, which enhances the performance of PEMFC. The results are consistent with that of OCVs. The change of S_{EAS} with time displays an adverse effect on the performance of PEMFC with the thickness decrease of Nafion® film, which results in that the evident decrease of the polarization curves in PEMFC was not found. The experimental data indicate that Pt/C catalyst and catalyst layer in the cathode evidently decay due to a marked decrease of 'triple-phase boundaries' where the electrolyte, reactants, and electrically connected catalyst particles contact together. Consequently, the performance decay of PEMFC mainly derives from the change of the cathode.

Fig. 6 shows TEM micrographs of Pt/C catalysts before and after the life test. Fig. 6A is a TEM micrograph of new catalyst and Fig. 6B and C are TEM micrographs of anodic and cathodic Pt/C catalysts after the life test, respectively. The dark black portions are Pt grains, and the gray portions are carbon support grains. It can be seen that the dispersion of new catalyst is very even without agglomeration, and its size is very small. The dispersion of the anodic catalyst after the test is relatively even, but its size evidently increases. However,

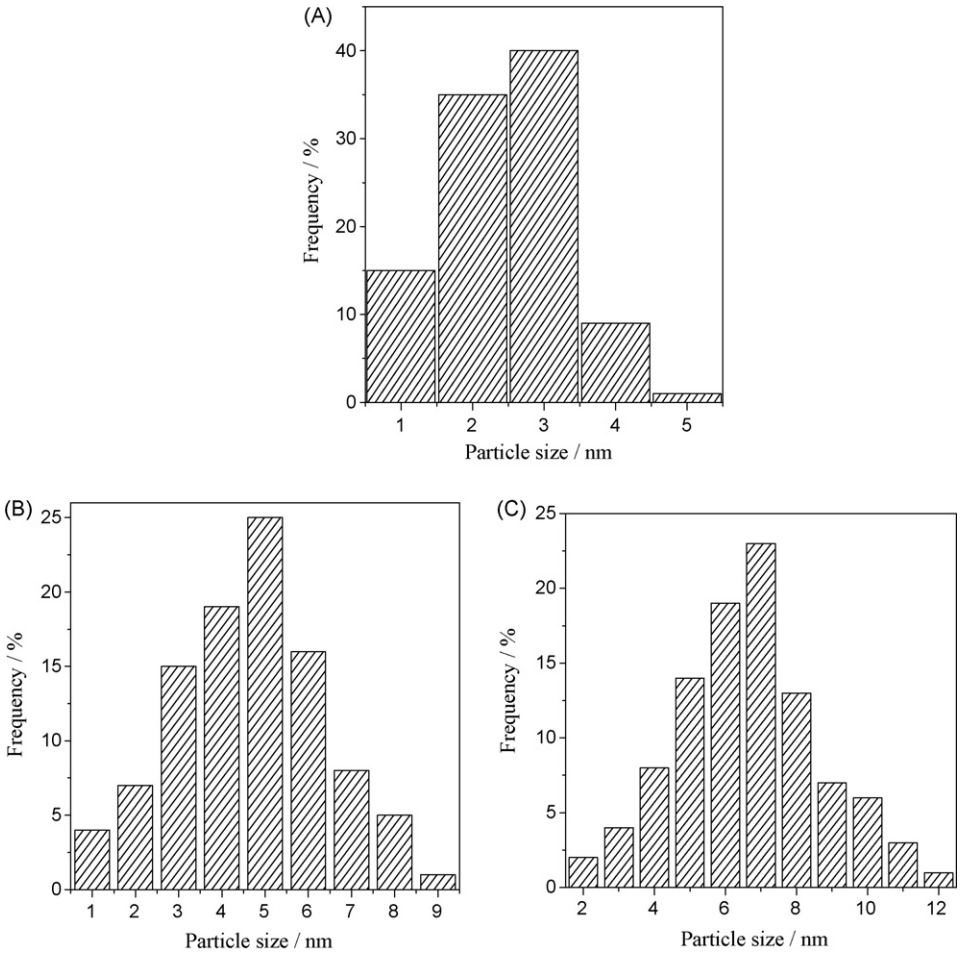

Fig. 7. Size distribution of nanoparticles of new Pt/C (A), anodic (B), and cathodic (C) Pt/C catalysts after life test.

the dispersion of the cathodic one after the test is uneven with a certain extent of agglomeration. Its size markedly increases. Kim and coworkers [29] studied the stability of Pt-based ternary alloy as cathodic catalysts for PEMFC. They also found the particle size of Pt-based ternary alloy catalysts increased by about 0.5 nm after 500 h of operation.

From the histograms of the particle sizes (see Fig. 7A for the new Pt/C catalyst, and Fig. 7B and C for the anodic and cathodic Pt/C ones after the life test, respectively), it is easy to pinpoint the peak particle sizes at around 3 nm, 5 nm, and 7 nm for the new Pt/C, anodic and cathodic Pt/C catalysts after the life test, respectively. From the particle distribution (i.e. from 1 nm to 5 nm for the new Pt/C nanoparticles, and from 1 nm to 9 nm for the anodic Pt/C and from 2 nm to 12 nm for the cathodic Pt/C catalyst after the life test) the more detailed estimation results of the average particle size of 2.6 nm for the new Pt/C nanoparticles, and those of 5.1 nm and 7.3 nm for the anodic and cathodic Pt/C catalysts after the life test, respectively, were computed from TEM measurements of particles with a series of definite particle diameters, coded individually with numbers, by using Eq. (2) [21] as follows:

$$\bar{d}_n = \frac{\sum_{i=1}^{n} d_i}{n} \quad (2)$$

where $\bar{d}_n$ is the averaged diameter of metal particles in nanometer, n the total number of the used codes, d_i the ith coded diameter. The results are similar to those of XRD. Simultaneously, the increases of particle size of Pt/C catalysts are consistent with their decreases of S_{EAS}. Comparing with the original one (Fig. 7A), the Pt particle size distributions are changed for the anodic and cathodic catalysts after the life test. The number of Pt particles with small diameters (1 nm) largely decreases or disappears, and larger Pt particles (larger than 6 nm) appear. It can be described that smaller Pt particles were "swallowed up" by the larger ones through the migration of smaller Pt particles on the carbon surface [30,31] or through the Pt ions (e.g., Pt^{2+}) dissolution/redeposition processes [27,32].

4. Conclusion

Measurements with XRD, SEM, TEM, and S_{EAS} of Pt/C catalysts at both electrodes were successfully applied to investigate the performance decay of a single PEMFC. The initial peak power densities firstly increased and then slightly decreased with the test time. Compared with anodic potentials, the cathodic ones are relatively high, which has a strong adverse effect on cathodic catalyst. The S_{EAS} of Pt/C catalysts in both electrodes initially augmented and then decreased markedly with time. The rate of S_{EAS} loss of cathodic catalyst is much higher than that of anodic one. The decreases of S_{EAS} and utilization of cathodic catalyst are the main factors affecting the performance decay of PEMFC. The thickness of Nafion® film also decreased with working time. The Nafion® film was thinned by about 4 μm after a working time of 2250 h. The particle size of cathodic catalyst is much bigger than that of anodic one. The increase of the particle size of Pt/C catalyst followed along with the dissolution/redeposition mechanism. The degradation of cathodic catalyst for oxygen electroreduction was one of the main factors affecting the performance decay of PEMFC.

Acknowledgements

This work is supported financially by the National Natural Science Foundation of China (Grant No. 20606007), Postdoctoral Science-Research Developmental Foundation of Heilongjiang Province of China (LBH-Q07044), the Scientific Research Foundation for the Returned Overseas Chinese Scholars, State Education Ministry (2008), and Harbin Innovation Science Foundation for Youths (2007RFQXG042).

References

[1] U.H. Jung, K.T. Park, E.H. Park, S.H. Kim, J. Power Sources 159 (2006) 529–532.
[2] Y. Bultel, K. Wiezell, F. Jaouen, P. Ozil, G. Lindbergh, Electrochim. Acta 51 (2005) 474–488.
[3] E.A. Cho, U.S. Jeon, S.A. Hong, I.H. Oh, S.G. Kang, J. Power Sources 142 (2005) 177–183.
[4] J. Scholta, N. Berg, P. Wilde, L. Jörissen, J. Garche, J. Power Sources 127 (2004) 206–212.
[5] S.H. Lee, J. Han, K.Y. Lee, J. Power Sources 109 (2002) 394–402.
[6] D. Candusso, F. Harel, A. De Bernardinis, X. Francois, M.C. Péra, D. Hissel, P. Schott, G. Coquery, J.M. Kauffmann, Int. J. Hydrogen Energy 31 (2006) 1019–1030.
[7] Y.T. Seo, D.J. Seo, J.H. Jeong, W.L. Yoon, J. Power Sources 163 (2006) 119–124.
[8] P. Konig, A. Weber, N. Lewald, T. Aicher, L. Jorissen, E. Ivers-Tiffee, R. Szolak, M. Brendel, J. Kaczerowski, J. Power Sources 145 (2005) 327–335.
[9] D.O. Energy (Ed.), Basic Research Needs for the Hydrogen Economy, Report of the Basic Energy Science Workshop on Hydrogen Production, Storage and Use Prepared by Argonne National Laboratories, Rockville, Maryland, 2003, pp. 53–60.
[10] D. Liu, S. Case, J. Power Sources 162 (2006) 521–531.
[11] B. Merzouguia, S. Swathirajanb, J. Electrochem. Soc. 153 (2006) A2220–A2226.
[12] J.L. Qiao, M. Saito, K. Hayamizu, T. Okada, J. Electrochem. Soc 153 (2006) A967–A974.
[13] S.Y. Ahn, S.J. Shin, H.Y. Ha, S.A. Hong, Y.C. Lee, T.W. Lim, I.H. Oh, J. Power Sources 106 (2002) 295–303.
[14] K.A. Mauritz, R.B. Moore, Chem. Rev. 104 (2004) 4535–4585.
[15] T.A. Zawodzinski, D. Schiraldi, J. Macromol. Sci. C: Poly. Rev. 46 (2006) 215–217.
[16] H. Tang, Z.G. Qi, M. Ramani, J.F. Elter, J. Power Sources 158 (2006) 1306–1312.
[17] W.M. Chen, G.Q. Sun, J.S. Guo, X.S. Zhao, S.Y. Yan, J. Tian, S.H. Tang, Z.H. Zhou, Q. Xin, Electrochim. Acta 51 (2006) 2391–2399.
[18] L. Li, Y.C. Xing, J. Electrochem. Soc. 153 (2006) A1823–A1828.
[19] D.A. Stevens, M.T. Hicks, G.M. Haugen, J.R. Dahn, J. Electrochem. Soc. 152 (2005) A2309–A2315.
[20] X. Wang, W.Z. Li, Z.W. Chen, M. Waje, Y.S. Yan, J. Power Sources 158 (2006) 154–159.
[21] P.J. Ferreira, G.J. la O', Y. Shao-Horn, D. Morgan, R. Makharia, S. Kocha, H.A. Gasteiger, J. Electrochem. Soc. 152 (2005) A2256–A2271.
[22] A. Pozio, M.D. Francesco, A. Cemmi, F. Cardellini, L. Giorgi, J. Power Sources 105 (2002) 13–19.
[23] J.R. Yu, T. Matsuura, Y. Yoshikawa, M.N. Islam, M. Hori, Electrochem. Solid-State Lett. 8 (2005) A156–A158.
[24] J. Xie, D.L. Wood III, D.M. Wayne, T.A. Zawodzinski, P. Atanassov, R.L. Borupa, J. Electrochem. Soc. 152 (2005) A104–A113.
[25] Z.B. Wang, H. Rivera, X.P. Wang, H.X. Zhang, P.X. Feng, E.A. Lewis, E.S. Smotkin, J. Power Sources 177 (2008) 386–392.
[26] T. Kinumoto, M. Inaba, Y. Nakayama, K. Ogata, R. Umebayashi, A. Tasaka, Y. Iriyama, T. Abe, Z. Ogumi, J. Power Sources 158 (2006) 1222–1228.
[27] M.S. Wilson, F.H. Garzon, K.E. Sickafus, S. Gottesfeld, J. Electrochem. Soc. 140 (1993) 2872–2877.
[28] M. Prasanna, E.A. Cho, T.-H. Lim, I.-H. Oh, Electrochim. Acta 53 (2008) 5434–5441.
[29] A. Seo, J. Lee, K. Han, H. Kim, Electrochim. Acta 52 (2006) 1603–1611.
[30] H.R. Colon-Mercado, H. Kim, B.N. Popov, Electrochem. Commun. 6 (2004) 795–799.
[31] Y.Y. Shao, G.P. Yin, Y.Z. Gao, P.F. Shi, J. Electrochem. Soc. 153 (2006) A1093–A1097.
[32] R.M. Darling, J.P. Meyers, J. Electrochem. Soc. 150 (2003) A1523–A1527.